ELSEVIER

Catalysis Today 27 (1996) 297–305

CATALYSIS TODAY

# Selective removal of NO by absorption in mixed oxide catalysts

Koichi Eguchi *, Mitsunori Watabe, Masato Machida, Hiromichi Arai

*Department of Materials Science and Technology, Graduate School of Engineering Sciences, Kyushu University, Kasuga, Fukuoka 816, Japan*

**Abstract**

Selective removal of NO by binary oxide systems of Ba–Cu, Mn–Y and Mn–Zr was investigated. These mixed oxides were effective in removing NO at 200–300°C by absorption in the solid as nitrate. The reaction was initiated by oxidation of NO, which was promoted in the presence of $O_2$, on Mn or Cu sites. Then, the oxidized species were stored in the solid as nitrate ions on Ba, Y or Zr sites. An infrared band of $NO_3^-$ was observed in the Mn–Y and Mn–Zr oxide samples after NO absorption treatment. Absorbed NO could be released on heating or by reduction of the absorbed species. Although the absorption was hindered by coexisting $CO_2$ for the Ba–Cu and Mn–Y oxide systems, the NO absorption in the Mn–Zr oxide was hardly affected by $CO_2$ and was enhanced in the presence of $H_2O$. Supported Mn–Zr oxide on alumina was effective in the removal of NO and attained a high absorption amount per Zr atom.

*Keywords*: Nitrogen oxide; Mixed oxide catalysts

## 1. Introduction

Removal of $NO_x$ from the atmosphere is important in solving the acid rain and other air pollution problems. Catalytic processes have been widely investigated for $NO_x$ removal. Selective catalytic reduction (SCR) of $NO_x$ with hydrocarbons has been actively investigated recently by many researchers. Cu-exchanged ZSM-5 [1,2], metallosilicates [3], alumina [4] and metal-exchanged zeolites [5–7] have been reported to be active for this reaction. But the SCR with hydrocarbons has not yet been commercialized due to some problems concerning the catalyst deactivation by the coexisting gases, such as $H_2O$ and $SO_2$. This difficulty is, to some extent, related with very dilute concentration of $NO_x$ in exhaust gases. One possible answer to overcome this difficulty would be to separate dilute $NO_x$ from the gas mixture before catalytic $NO_x$ conversion. The separation process for $NO_x$ suppresses the degradation of the catalysts by supplying concentrated NO without poisonous components to the catalyst. A similar concept has been commercialized in the $NO_x$ storage reduction catalyst proposed by the research group of Toyota motor [8]. The 3-way catalyst was combined with a $NO_x$ storage material such as barium oxide in their catalyst. Nitrogen oxides are first stored in the solid in the oxidized form during cruising with an automobile in lean-burn condition. Then, the stored $NO_x$ is released and reduced by the 3-way catalyst when the atmosphere was changed intermittently to the stoichiometric air/fuel ratio. This application suggests an importance of the investigation of a reversible NO ab- or adsorbate in the catalytic conversion of $NO_x$. Several mixed oxide

* Corresponding author.


*SSDI* 0920-5861(95)00200-6

systems, such as Y–Ba–Cu–O and Y–Sr–Co–O, were reported to be active for removal of NO by absorption in the solid [9,10]. We also have reported that some mixed oxides containing Ba–Cu–O and Ba–Cu–Mn–O are active for reversible absorption of NO in an oxidizing atmosphere [11,12]. Nitrogen monoxide is oxidized on the oxide surface then retained in solid as nitrate. The absorbed $NO_x$ can be released on heating or by reducing nitrate ion. The present investigation aims at development of NO absorbent which can reversibly absorb dilute NO from exhaust gases and release concentrated NO by thermal or reduction treatment.

## 2. Experimental

### 2.1. Sample preparation

Mixed oxide samples were generally prepared by coprecipitation from the solution of corresponding nitrate mixture. For the preparation of Mn–Y and Mn–Zr oxides, calculated amounts of $Mn(NO_3)_3 \cdot 6H_2O$, $ZrO(NO_3)_2 \cdot 2H_2O$ and/or $Y(NO_3)_3 \cdot 6H_2O$ (Kishida Chemical, Guaranteed reagent grade) were dissolved in water. After adding ammonia water to the nitrate solution, the solution with precipitate was evaporated to dryness and then heated at 450°C for 6 h in air. The powder thus obtained was sieved to 10–20 mesh.

The Mn–Zr oxide was supported on alumina by the impregnation process. γ-Alumina powder (5.91 g) (Catalysis Soc. Jpn., ALO-4) was suspended in $2.52 \times 10^{-3}$ mol/l aqueous solution of $Mn(NO_3)_3$ and $ZrO(NO_3)_2$. The suspension was evaporated to dryness and the powder was treated with the same procedure as the unsupported samples.

### 2.2. NO removal experiment and characterization

Absorption and desorption experiments of NO were carried out in a flow system. Nitrogen monoxide was diluted in He or $N_2$ and mixed with $O_2$ before supplying to a quartz tube reactor. The absorption and desorption characteristics of NO was tested in a temperature range from 200 to 700°C at a contact time of 0.6–1.0 g s $cm^{-3}$. The concentration of $NO_x$ was analyzed with a chemical luminescence type $NO_x$ meter (Shimadzu, NOA305). The effluent gas was generally passed through a carbon catalyst to reduce $NO_2$ when analyzing a $NO + NO_2$ concentration. Only when NO concentration was necessary, the sample gas was directly introduced to the $NO_x$ meter. The gaseous composition of inlet and outlet mixtures was also analyzed by gas chromatography.

The absorption state of $NO_x$ was recorded with an FT–IR spectrometer (Shimadzu, FT–IR 8200D) using the KBr method. The phase in the sample was identified by an X-ray diffraction spectrometer (Rigaku, RINT-1400) equipped with a rotating Cu anode and a monochromator. Thermal gravimetric analysis (TGA) of the decomposition of nitrate salts was carried out by using a Shimadzu TGA-40H.

## 3. Results and discussion

### 3.1. Removal of NO by Ba-based oxides

The activity of Ba-based mixed oxides for the removal of NO is summarized in the upper half of Table 1. System Ba–Cu–O completely removed 0.1% NO in $N_2$ at 200–300°C. In the presence of gaseous $O_2$, removal of NO was enhanced for all the samples. Whereas the system Ba–Cu–O consists of $BaCuO_{2.1}$ and $BaCuO_{2.5}$, these phases disappeared after the NO removal, and $Ba(NO_3)_2$ and CuO appeared. On heating above 500°C, the initial phases recovered with releasing $NO_x$ absorbed. The enhancement of the NO removal by $O_2$ strongly suggests that the removal proceeds via oxidation of NO. Whereas the single phase $BaCuO_{2.1}$ is essentially inactive, a mixture of $BaCuO_{2.1}$/CuO removes NO efficiently. Actually, CuO readily oxidizes NO to $NO_2$. The present NO removal is, therefore, attributed to catalytic oxidation and subsequent absorption of NO, probably

Table 1
Removal of NO by various mixed oxides[a]

| Oxide | NO removal (%) | |
|---|---|---|
| | $O_2$ (0%)[b] | $O_2$ (10%)[c] |
| Ba–Cr–O[d] | 8.0 | 18.6 |
| Ba–Mn–O[d] | 2.8 | 7.9 |
| Ba–Fe–O[d] | 6.9 | 10.7 |
| Ba–Co–O[d] | 18.6 | 33.3 |
| Ba–Ni–O[d] | 1.4 | 2.5 |
| Ba–Cu–O[d] | 100.0 | 100.0 |
| Mn–Fe–O[e] | 11.9 | 37.4 |
| Mn–Mo–O[e] | 5.9 | 15.2 |
| Mn–Zr–O[e] | 100.0 | 100.0 |
| Zr–Cu–O[e] | 2.7 | 27.0 |

[a] Reaction temperature, 200°C. NO removal is obtained after 20 min of service.
[b] NO 0.1%.
[c] NO 0.09%, $O_2$ 10%.
[d] Calcined at 750°C. Balanced with $N_2$, $W/F = 0.6$ g s cm$^{-3}$.
[e] Calcined at 450°C. Balanced with He, $W/F = 1.0$ g s cm$^{-3}$.

forming nitrate-related compounds in the oxides.

The activity of $BaCuO_{2.1}/CuO$ for NO is, however, seriously damaged by coexisting $CO_2$ owing to formation of stable $BaCO_3$. On the other hand, the activity for $NO_2$ was rather insensitive to $CO_2$, implying that the deactivation by $CO_2$ can be prevented by using oxidizing catalysts stronger than CuO. As seen in Fig. 1, $BaCuO_{2.1}/MnO_2$ was exceedingly tolerant to $CO_2$, and attained ca. 95% of NO removal even in the presence of 10% $CO_2$.

### 3.2. Absorption of NO by Mn–Y oxide

The absorptive property of NO was also investigated for the Mn–Y oxide system, since yttrium nitrate, $Y(NO_3)_3$, is relatively stable among nitrates. Dilute NO (900 ppm) and $O_2$ (10 vol-%) was supplied to the Mn–Y oxides with 3 different compositions. The time course of the absorption curve is shown in Fig. 2. This mixed oxide system with Mn/Y = 1 also absorbed a large amount of NO as shown in Fig. 2. The initial removal of 3 samples was 100%. The amount of absorption was 0.054 mol NO/mol Y for the sample with Mn/Y = 1; i.e., a relatively large fraction of Y is participating in the absorption reaction.

The X-ray diffraction patterns with the surface areas of the Mn–Y system are shown in Fig. 3. The Mn–Y oxide with Mn/Y = 3 and Mn/Y = 1/3 exhibited very sharp diffraction lines attributed to $MnO_2$ and $Y_2O_3$ phases, respectively, after heating at 450°C. However, the diffraction pattern of Mn/Y = 1 consisted of very weak lines from $Y_2O_3$ and a broad halo after the same heating treatment. The surface area of the Mn/Y = 1 was highest among the three samples. It appears for the Mn–Y oxide with Mn/Y = 1 that the amorphous phase is effective in absorption of NO owing to the good mixing of Mn and Y components, and the large active surface. The present absorption reaction proceeds by oxidation of NO on the Mn site and subsequent absorption as $NO_3^-$ ion on the

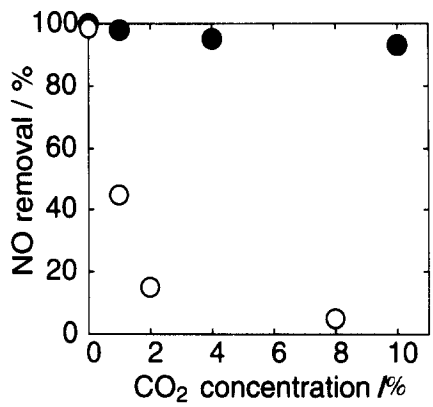


Fig. 1. The influence of coexisting $CO_2$ on NO removal by $BaCuO_{2.1}$. NO removal after 20 min of service. $T = 200$°C, $W/F = 0.6$ g s cm$^{-3}$. 0.1%–0.07% NO, 10% $O_2$, $N_2$ balance. ● $BaCuO_{2.1}/MnO_2$, ○ $BaCuO_{2.1}/CuO$.

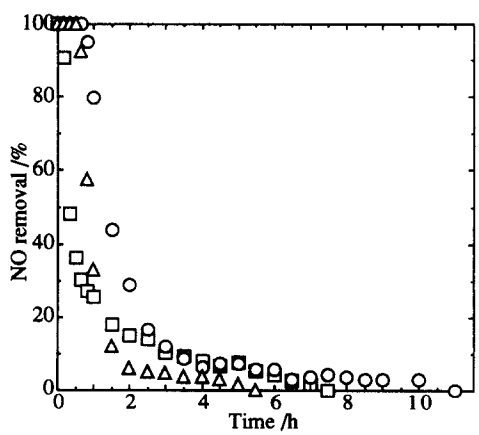


Fig. 2. Time course of NO absorption of Mn–Y oxides with different compositions. $T = 200$°C, $W/F = 1$ g s cm$^{-3}$, 900 ppm NO, 10% $O_2$, He balance. △ Mn/Y = 3, ○ Mn/Y = 1, □ Mn/Y = 1/3.

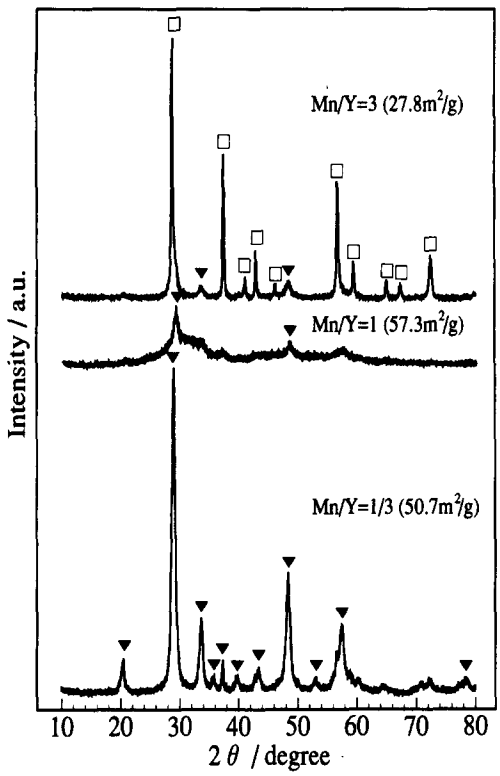


Fig. 3. X-Ray diffraction patterns and surface areas of Mn–Y oxides with different compositions after heating at 450°C. □ $MnO_2$, ▼ $Y_2O_3$.

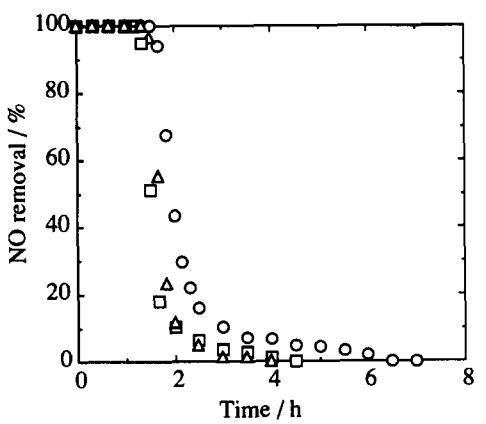


Fig. 4. Absorption curve of NO for Mn–Y oxide calcined at different temperatures for 6 h. 900 ppm NO, 10% $O_2$, He balance, $W/F = 1$ g s $cm^{-3}$, reaction temperature: 200°C. calcination temperature: ○ 450°C, □ 550°C, △ 650°C.

Y site; therefore the reaction is expected to occur at the boundary between the Mn- and Y-phases. Furthermore, the reaction starts from the surface and proceeds to the bulk accompanying the diffusion of reacting species through the formed nitrate layer, and hence a large surface area is naturally desired for the large absorption capacity.

An effect of heating pretreatment on the absorptive property of the Mn–Y oxide at Mn/Y = 1 is shown in Fig. 4. Heating at elevated temperatures resulted in a decrease in surface area of the sample, leading to the decrease in the overall absorption amount as summarized in Table 2.

X-Ray diffraction patterns of the Mn–Y oxide in Fig. 5 showed only weak lines for the $Mn_2O_3$ crystal except for a broad halo after heating at 450°C whereas sharp lines from Mn oxide and $Y_2O_3$ were obviously observed after heating at 550 and 650°C. The $MnO_2$ phase was dominant at 550°C, whereas the $Mn_2O_3$ phase existed mainly at 650°C, as was expected from the phase diagram of the Mn–O system. The coexistence of the two

Table 2
Absorption capacity and surface area of Mn–Y oxide calcined at different temperatures

| Temperature (°C) | 450 | 550 | 650 |
|---|---|---|---|
| Surface area ($m^2\ g^{-1}$) | 57.3 | 37.3 | 33.0 |
| Absorption capacity ($10^{-4}$ mol $g^{-1}$) | 2.82 | 2.45 | 1.70 |
| Mol absorbed NO/mol Y | 0.054 | 0.047 | 0.033 |

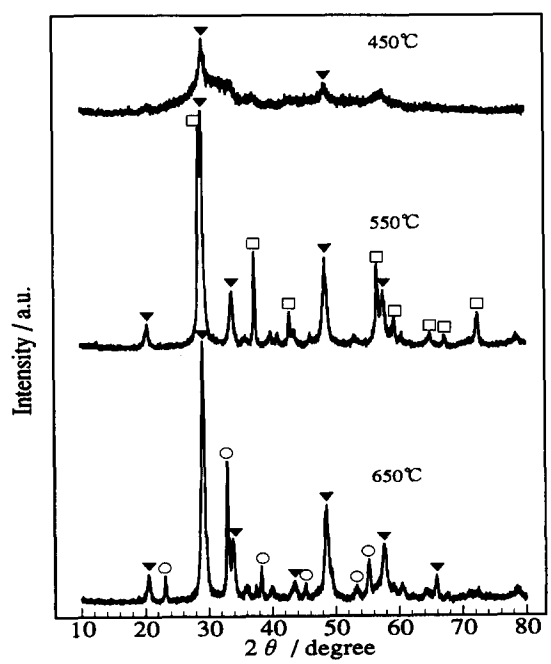


Fig. 5. X-Ray diffraction patterns of Mn–Y oxides (Mn/Y = 1) heated at different temperatures. ○ $Mn_2O_3$, □ $MnO_2$, ▼ $Y_2O_3$.

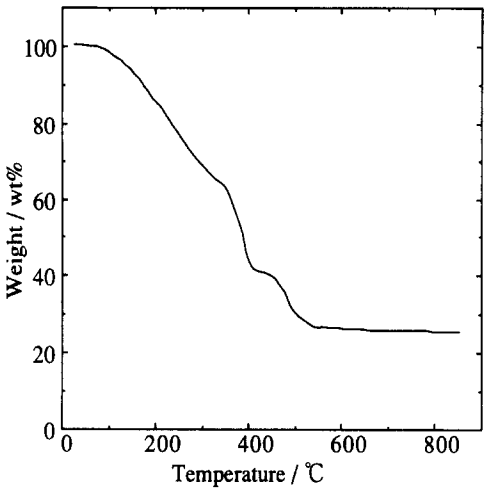


Fig. 6. Thermogravimetric analysis of $Y(NO_3)_3 \cdot 6H_2O$ in $N_2$. Heating rate: 10°C $min^{-1}$, $N_2$ flow rate: 8 ml $min^{-1}$.

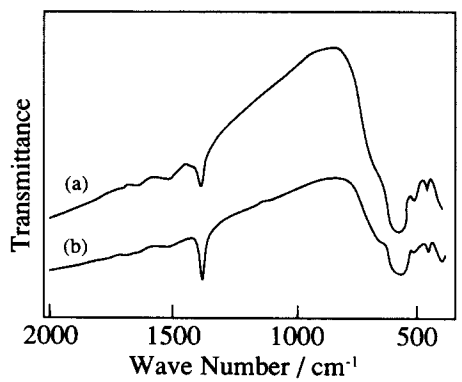


Fig. 7. FT–IR spectra of Mn–Y oxide (a) after heating in air at 450°C and (b) after absorption of NO at 200°C. Mn–Y oxide: Mn/Y = 1.

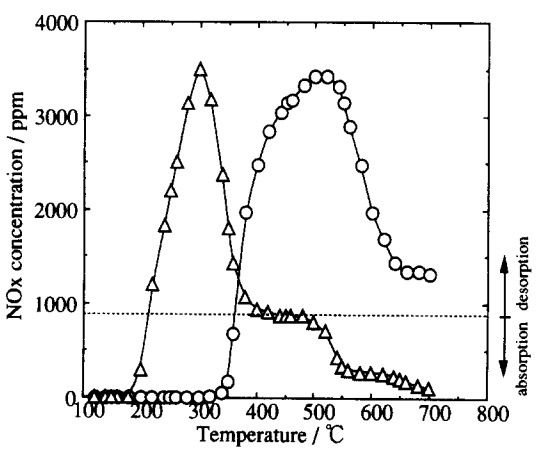


Fig. 8. Absorption–desorption curve of NO for Mn–Y oxide during programmed heating in different atmospheres. Mn–Y oxide: Mn/Y = 1; heated at 450°C for 6h. ○ 900 ppm NO + 10% $O_2$, △ 900 ppm NO + 1500 ppm $C_3H_8$, He balance, $W/F = 1$ g s $cm^{-3}$. - - - initial concentration of NO, heating rate: 5°C /min.

phases in the sample indicates that the separated Mn oxide and $Y_2O_3$ phases are in equilibrium at this composition, thus, the crystallization of the oxide leads to the deterioration of the absorption performance not only by a decrease in surface area but also by the phase separation.

A gravimetric analysis of $Y(NO_3)_3 \cdot 6H_2O$ was carried out to clarify the decomposition behavior and its relation with NO absorption–desorption properties (Fig. 6). Several complex weight losses were observed from room temperature to 500°C. The decomposition of $Y(NO_3)_3$ completed at ca. 530°C in $N_2$ atmosphere. The weight decrease almost agreed with that assumed from the following reaction.

$$Y(NO_3)_3 \cdot 6H_2O \rightarrow \frac{1}{2}Y_2O_3 + 3NO_2 + \frac{3}{4}O_2 + 6H_2O \quad (1)$$

Infrared spectra were recorded before and after the absorption treatment of NO to observe the absorbed species (Fig. 7). The IR band for the Mn–Y oxide before the absorption treatment after heating at 450°C exhibited a small band at 1384 $cm^{-1}$. This band is assigned to the $\nu_3$ stretching band of the $NO_3^-$ ion which appears as the strongest peak in most nitrates [13], whereas other bending bands in the low wave number region could not be observed clearly due to the overlap with the band of the oxide. Since decomposition of the nitrate completed only at 530°C, as mentioned, residual nitrate ions are contained even after heat treatment at 450°C. This band was grown in its intensity after the absorption of NO at 200°C for 11 h. This confirms that the absorption proceeds with the formation of nitrate.

The gas with 900 ppm NO was supplied to the Mn–Y oxide under programmed heating schedule (10°C/min). Fig. 8 shows the outlet concentration of NO as a function of temperature, where the broken line is the initial concentration of NO (900 ppm). Nitrogen monoxide was completely removed from the gas phase from 100 to 350°C in the case of the gas with 10% $O_2$. As has been explained, this removal is attributed to the absorp-

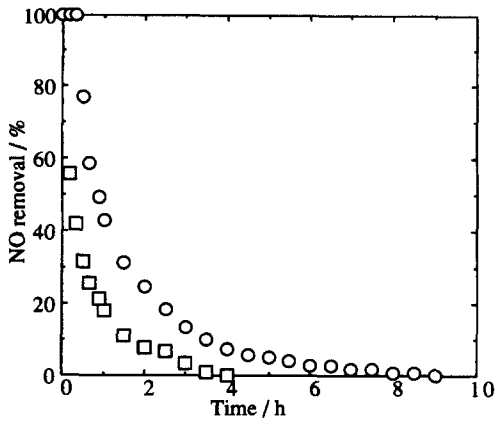


Fig. 9. Effect of $CO_2$ on absorption curve of NO in Mn–Y oxide (Mn/Y = 1). $T$ = 200°C, $W/F$ = 1 g s cm$^{-3}$. ○ 800 ppm NO, 10% $O_2$, He balance. □ 800 ppm NO, 10% $O_2$, 10% $CO_2$, He balance.

tion of $NO_x$ species in the solid bulk. Heating of the sample above 350°C led to desorption of NO from oxide, thus, the outlet concentration far exceeded the initial value. At elevated temperatures, the desorption curve approached the initial concentration level as neither absorption nor desorption proceeded.

The absorption of NO by the Mn–Y oxide also proceeded in the presence of $C_3H_8$ below 200°C as shown in Fig. 8. However, a sharp desorption peak was observed from 200°C. The temperature at the start of the desorption was significantly lowered as compared with the case NO + $O_2$. The desorption finished at 400°C. Then, the NO concentration again decreased below the initial concentration level and reached zero at 700°C. The NO removal in this region was not due to absorption, but to the catalytic reduction of NO with

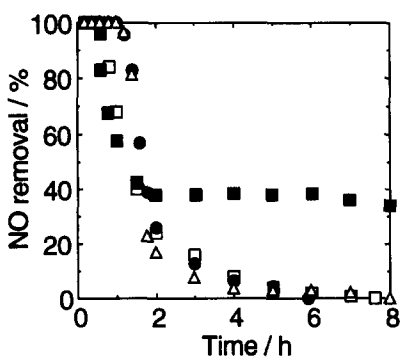


Fig. 10. NO removal by Mn–Zr oxide at 200°C. 0.1% NO, 10% $O_2$, $W/F$ = 1.0 g s cm$^{-1}$. ● 1st run, △ 2nd run after recovery at 400°C, □ 1st run with 10% $CO_2$, ■ 1st run with 0.6% $H_2O$. He balance.

$C_3H_8$. Produced $N_2$ was detected by the gas phase analysis. The reversibility of absorption and desorption is a most desirable property for the present absorption system. Desorption of NO from the solid proceeded on heating the sample, as mentioned. Another method for desorption is the reduction of the absorbed $NO_x$ species in the solid. Nitrate ions, $NO_3^-$, are expected to be strongly held in the solid due to their high polarity, but the reduction of these species weakens the bonding and promotes the desorption of NO.

The purpose of the present study is the removal of $NO_x$ from combustion exhaust. The effect of coexisting $CO_2$ was investigated. The absorption curves with or without $CO_2$ are shown in Fig. 9. In the gas with $CO_2$, the NO removal began to decrease from the start of the gas supply, thus, resulting absorption capacity was obviously lowered. The molar ratio of the overall absorption was 0.015 mol NO/mol Y for $CO_2$ containing atmosphere, which was far below the molar ratio of absorption obtained in the $CO_2$ free atmosphere. The deterioration with $CO_2$ results from the strong basicity of the rare earth element Y. Carbon dioxide absorbs competitively with $NO_x$ and carbonate ions form more stable bondings with Y than nitrate ions. But the use of components with weaker basicity which form thermally stable nitrate is one possible method to design the absorbent for $NO_x$.

### 3.3. Removal of $NO_x$ by Mn–Zr oxide

The material selection for the absorption site of the nitrate ion was started from the alkaline earth oxide and then proceeded to rare earth oxide in the present study. Since these oxides are revealed to form too strong bondings with $CO_2$, we tried to develop materials without alkaline earth or rare earth oxides. The NO removal was examined for several oxide materials containing Mn and/or Zr. As shown in Table 1, the Mn–Fe, Mn–Mo, Mn–Zr and Mn–Cu oxides exhibited the relatively high removal of NO. The Mn–Zr oxide exhibited the highest NO removal both with and without $O_2$. The time course of the NO removal for the Mn–Zr oxide is shown in Fig. 10. The total amount of

NO removed during 6 h of the experiment was 14.7 $cm_3$ (STP)/g which corresponds to 0.08 mol NO/mol Zr. As similar to the Ba- and Y-based systems, the NO absorption is suggested to accompany the oxidation of NO on the surface to $NO_2$. It was confirmed that the absorption curve and overall uptake for $NO_2$ were almost the same as those for NO. These two gas species are expected to be held in the oxide with the same mechanism. The overall rate of absorption is not affected by the rate of oxidation from NO to $NO_2$.

Nitrogen monoxide removed from the gas phase was desorbed on heating to 400°C in He. After the complete NO absorption, after 60 min, the amount of desorbed NO (0.044 mol/mol Zr) almost agreed with that of absorbed (0.047 mol/mol Zr), indicating that the absorption and desorption of NO by the Mn–Zr oxide is almost reversible. The absorption capacity of the Mn–Zr oxide is higher than that of the Mn–Y oxide but was lower than that of $BaCuO_{2.1}/MnO_2$. The capacity of the Mn–Zr oxide in the second run after the recovery at 400°C was nearly the same as the initial value as shown in Fig. 10, and the oxide retained almost the same capacity even in the fifth run. Whereas practically neither single oxide of $MnO_x$ nor $ZrO_2$ absorbs NO, the combination of them markedly enhances the activity and attained the maximum removal at the composition of Mn/Zr = 1. At this composition, only a weak diffraction line of $Mn_2O_3$ was observed with a broad and dominant halo pattern from an amorphous phase, and also the specific surface area became the maximum.

The absorption behavior was also examined in the presence of $CO_2$ and $H_2O$. The absorption curve and the total absorption capacity of the Mn–Zr oxide were hardly affected even in the presence of 10% $CO_2$ as shown in Fig. 10. This tolerance to $CO_2$ is contrasting with the Cu–Ba and Mn–Y systems and appears to be related with the basicity of the absorption site for nitrate ions. So far, we developed the absorption site of nitrate in the decreasing order of basicity starting from the alkaline earth oxide and then the rare earth oxide to the group IV metal oxide. The strong basicity

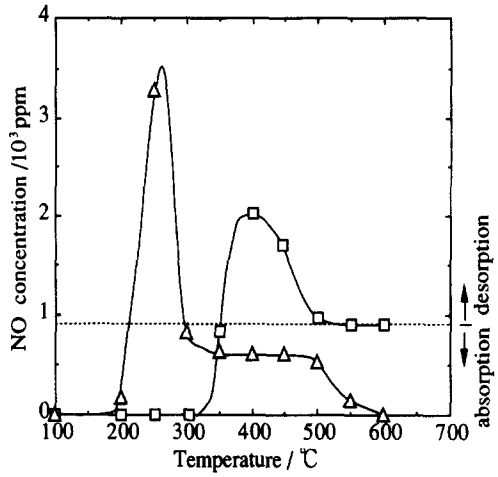


Fig. 11. Absorption–desorption curve of NO for Mn–Zr oxide during programmed heating in different atmospheres. Mn–Zr oxide: Mn/Zr = 1; heated at 450°C for 6h. □ 900 ppm NO + 10% $O_2$, △ 900 ppm NO + 1500 ppm $C_3H_8$, He balance, $W/F = 1$ g s $cm^{-3}$. - - - initial concentration of NO.

results in stable bonding with $CO_2$ through formation of carbonate and, hence, the NO absorption becomes irreversible in the presence of $CO_2$. The control of basicity is an important factor in the design of the absorption site for oxidized $NO_x$ species.

Although the NO absorption in the presence of $H_2O$ during the initial 130 min was scarcely affected, the absorption rate remains quite high even after 3 h NO removal as seen in Fig. 10. The overall amount of absorption was obviously enhanced by the coexisting $H_2O$. The water molecules appear to stabilize absorbed nitrate ions through hydration and to facilitate gas–solid reaction by promoting the diffusion of the gas molecules.

The gas with 900 ppm NO was supplied to the Mn–Zr oxide under programmed heating schedule (10°C/min). Fig. 11 shows the outlet concentration of NO as a function of temperature where the broken line is the initial concentration of NO (900 ppm). The absorption–desorption behavior during heating was basically the same as in the case of the Mn–Y oxide. Nitrogen monoxide was completely removed from the gas phase from 200 to 300°C in the case of the gas with 10% $O_2$. Heating of the sample at the elevated temperatures of 320–500°C led to desorption of NO from oxide, thus

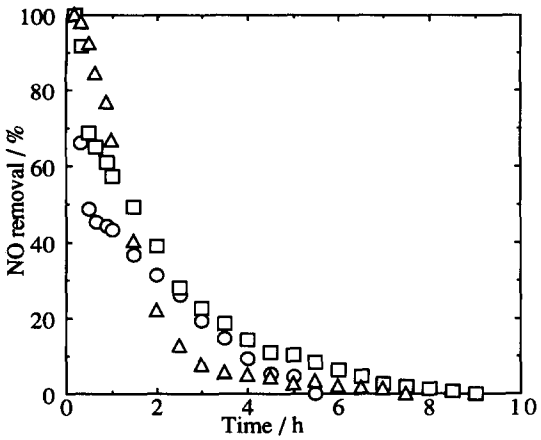


Fig. 12. Time course of NO absorption in Mn–Zr–O/$Al_2O_3$. $T$=200°C, $W/F$=1 g s $cm^{-3}$. 900 ppm NO, 10% $O_2$, He balance, loading of Mn–Zr oxide: ○ 3.5 wt.-%, □ 9.5 wt.-%, △ 30 wt.-%.

the outlet concentration far exceeded the initial value. Neither absorption nor desorption proceeded above 500°C.

The amorphous phase of the Mn–Zr oxide, which was formed after heating this oxide system at 450°C, was effective for NO removal probably due to the good mixing of Mn and Zr oxide species. Crystallization of the oxide at elevated temperatures accompanies the phase separation of the two components, resulting in loss of absorptive capacity. The infrared analysis of the Mn–Zr oxide after absorption treatment of NO indicated a sharp absorption band centered at 1384 $cm^{-1}$ which is attributed to $(NO_3)^-$ [13]. Zirconium oxide nitrate, $ZrO(NO_3)_2$, also possesses a strong absorption band at 1384 $cm^{-1}$. Since the absorption and desorption was reversible, the oxide solid was recovered on heating at 400°C, releasing the concentrated $NO_x$.

Table 3
Surface area and cumulative amount of NO absorption for Mn–Zr–O/$Al_2O_3$

| Loading (wt.-%) | 0[a] | 3.5 | 9.5 | 30 | 100[b] |
|---|---|---|---|---|---|
| Surface area ($m^2\ g^{-1}$) | 156.9 | 165.5 | 159.4 | 140.9 | 185.4 |
| NO absorption capacity ($10^{-4}$ mol $g^{-1}$) | 0 | 2.19 | 2.93 | 2.31 | 4.06 |
| Mol absorbed NO/mol Zr | 0 | 1.21 | 0.62 | 0.15 | 0.082 |

[a] $Al_2O_3$.
[b] Mn–Zr oxide.

The absorption of NO by the Mn–Zr oxide also proceeded in the presence of $C_3H_8$ below 200°C as shown in Fig. 11. However, a sharp desorption peak was observed from 220°C. The temperature at the start of the desorption was significantly lowered as compared with the case of NO + $O_2$. The desorption finished at 300°C. Then, the NO concentration again decreased below the initial concentration level and reached zero at 600°C due to the reduction of NO with $C_3H_8$. Produced $N_2$ was detected by the gas phase analysis. The reversibility of absorption and desorption is a most desirable property of the present absorption system. Desorption of NO absorbed in the solid proceeded on heating as mentioned. The reduction treatment of the absorbed $NO_x$ species is also effective in recovery of the oxide.

The Mn–Zr oxide is a reversible absorbent of NO in exhaust gas with a large absorption capacity, reversibility of absorption–desorption and tolerance to $CO_2$ and $H_2O$, as mentioned so far. The improvement of absorption capacity was further investigated by supporting this oxide on γ-alumina (Fig. 12). The increase in surface to volume ratio is expected to enhance both absorption capacity and rate, since the absorption initiates from the surface. Practically only a limited part of oxide within a certain depth from the surface can participate in the absorption, because the nitrate formation may become diffusion-limited in the formed layer. The weight of Mn–Zr–O/$Al_2O_3$ was fixed, but loading of the active component was changed in this experiment. The supported Mn–Zr oxide also exhibited high removal of NO and the decrease in amount of the active Mn–Zr–O component did not affect the absorption curve so seriously. The surface areas, absorption capacity and molar ratio of absorption for the supported and unsupported Mn–Zr oxide, and alumina are summarized in Table 3. The surface area was lower for the supported samples than for the unsupported Mn–Zr oxide, but the molar ratio of the NO absorption to Zr significantly increased. Thus, the Mn–Zr oxide works more effectively by supporting this oxide on alumina. The molar ratio of NO absorbed (1.21 mol/mol Zr) for 3.5% Mn–

$Zr–O/Al_2O_3$ indicates that most of the Zr ions participate in the absorption reaction. On the supported sample, fine particles of Mn oxide and Zr oxide are dispersed. This situation on the surface provides a large amount of the Mn oxide/Zr oxide interface which is active for the absorption of NO.

### *3.4. Comparison with other absorption system and concluding remarks*

The present investigation indicated that some mixed oxides are effective in removing dilute $NO_x$ in oxidizing atmosphere. Although several wet $NO_x$ removal processes have been proposed using alkaline solution or molten salt, the dry de$NO_x$ process is attractive due to ease in handling. The removal is initiated by oxidation of NO on the solid surface and subsequent absorption in the solid as the nitrate formation. The absorption and conversion to nitrate is regarded as a reverse reaction to form oxide from nitrate decomposition; and, hence, the reaction was almost reversible in all the oxides investigated in the present study. The repeated absorption–desorption was confirmed to be possible for every system in $CO_2$-free atmosphere. Some mixed metal oxides have been already reported to behave as $NO_x$ absorbents like the Mn–Zr oxide. Superconducting Y–Ba–Cu oxide [9], a $LaCoO_3$-based perovskite [10] and Ba–Cu oxide [11] exhibit high absorption capacities. These oxides also consists of an active component for catalytic oxidation of NO (Co and Cu) and absorption site (rare earth or alkaline earth ion). Therefore, the basic absorption phenomenon is regarded as the same as in the present case. Their absorption capacities are slightly larger than, but in the same order as, the present Mn–Zr oxide. The high absorption rate and capacity are generally attained using more basic components. The alkaline earth and rare earth is effective in this respect. However, the use of the bulk alkaline or rare earth compounds implies degradation by the formation of stable carbonate in the presence of $CO_2$. The weakened basicity, with using group IV metal, is inferior in the absorption rate and capacity to the case of alkaline or rare earth-containing systems. However, reversibility in the $CO_2$-containing atmosphere is the attractive advantage.

## Acknowledgements

One of the authors (K.E.) gratefully acknowledges the financial support from the Mitsubishi Foundation.

## References

[1] M. Iwamoto, H. Yahiro, Y. Shundo, O. Yu and N. Mizuno, Shokubai (Catalysts), 32 (1990) 430.
[2] W. Held, A. Koening, T. Richter and P. Puppe, SAE paper 900 496, 1990.
[3] E. Kikuchi, K. Yogo, S. Tanaka and M. Abe, Chem. Lett., (1991) 1063.
[4] Y. Kintaichi, H. Hamada, M. Tabata, M. Sasaki and T. Ito, Catal. Lett., 6 (1990) 239.
[5] Y. Li and J.N. Armor, Appl. Catal. B, 3 (1993) L1.
[6] K. Yogo, S. Tanaka, M. Ihara, T. Hishiki and E. Kikuchi, Appl. Catal. B, 2 (1993) L1.
[7] C. Yokoyama and M. Misono, Chem. Lett., (1992) 1669.
[8] N. Takahashi, H. Shinjoh, T. Iijima, T. Suzuki, K. Yamazaki, K. Yokota, H. Suzuki, N. Miyoshi and S. Matsumoto, Proc. 1st World Congr. Environ. Catal., (1995) 45.
[9] M. Misono and K. Kondo, Chem. Lett., (1991) 1001.
[10] M. Saitou, T. Tachi, H. Yamashita and H. Miyadera, Nippon Kagaku Kaishi, (1993) 703.
[11] M. Machida, K. Yasuoka, K. Eguchi and H. Arai, J. Solid State Chem., 91 (1991) 176.
[12] M. Machida, S. Ogata, K. Yasuoka, K. Eguchi and H. Arai, Proc. 10th Int. Congr. Catal., (1993) 2644.
[13] C.C. Addison and B.M. Gatehouse, J. Chem. Soc., (1960) 613.